Enhanced time response of 1-inch $LaBr_3$(Ce) crystals by leading edge and constant fraction techniques

V. Vedia[a,*], H. Mach[a,b,1], L.M. Fraile[a], J.M. Udías[a], S. Lalkovski[c,2]

[a] *Grupo de Física Nuclear, Facultad de CC. Físicas, Universidad Complutense, CEI Moncloa, ES-28040 Madrid, Spain*
[b] *National Centre for Nuclear Research, Division for Nuclear Physics, BP1, PL-00-681 Warsaw, Poland*
[c] *Faculty of Physics, University of Sofia, St. Kliment Ohridski, BG-1164 Sofia, Bulgaria*

Abstract

We have characterized in depth the time response of three detectors equipped with cylindrical $LaBr_3$(Ce) crystals with dimensions of 1-in. in height and 1-in. in diameter, and having nominal Ce doping concentration of 5%, 8% and 10%. Measurements were performed at ^{60}Co and ^{22}Na γ-ray energies against a fast BaF_2 reference detector. The time resolution was optimized by the choice of the photomultiplier bias voltage and the fine tuning of the parameters of the constant fraction discriminator, namely the zero-crossing and the external delay. We report here on the optimal time resolution of the three crystals. It is observed that timing properties are influenced by the amount of Ce doping and the crystal homogeneity. For the crystal with 8% of Ce doping the use of the ORTEC 935 CFD at very shorts delays in addition to the Hamamatsu R9779 PMT has made it possible to improve the $LaBr_3$(Ce) time resolution from the best literature value at ^{60}Co photon energies to below 100 ps.

Keywords: fast timing, inorganic scintillators, $LaBr_3$(Ce), Ce concentration, time resolution, Hamamatsu R9779, constant fraction discriminator, time walk

1. Introduction

High-density scintillators that exhibit fast response and good energy resolution are the preferred crystals in a number of applications such as gamma-ray spectroscopy, medical diagnosis and timing measurements. One of the fastest scintillators commercially available nowadays is $LaBr_3$(Ce) [1, 2, 3]. It has very good timing properties in addition to high γ-ray efficiency and good stopping power. Its energy resolution at 662 keV is measured to be as good as 2.8%, and its photon yield corresponds to 63 photons/keV [3], which is much higher than that of other inorganic scintillators [4].

Due to their superb properties, $LaBr_3$(Ce)-based detectors have been the option of choice since 2005 [5] for the application of the Advanced Time-Delayed (ATD) method, which was introduced as a HPGe-gated $\beta - \gamma$ electronic timing technique with ultra fast scintillators [6]. The ATD method allows the measurement of nuclear level lifetimes down to a few picoseconds by using the fast coincidences between the radiation populating and de-exciting a nuclear energy level [6, 7]. Nuclear level lifetimes are decisive observables in nuclear physics since they provide access to reduced transition probabilities between nuclear states, and therefore insight into the nuclear structure. Currently $LaBr_3$(Ce) crystals have become the standard detectors for *fast-timing* spectroscopy [8, 9, 10, 11].

The sensibility of the ATD method is directly determined by the time resolution of detectors in use, and therefore the best choice of crystal type ($LaBr_3$(Ce) in this case), size, shape and doping is required, together with the right selection of the coupling photosensor [12] is required. The optimization of the electronic circuit and the detector operation parameters is also needed to achieve the maximum performance [13, 14] of the setup.

In this paper we report on the time response of three $LaBr_3$(Ce) detectors equipped with 1-in. cylindrical

*Corresponding author
Email address: mv.vedia@ucm.es (V. Vedia)
URL: http://nuclear.fis.ucm.es (V. Vedia)

[1] During the preparation of the final version of this manuscript, our colleague Henryk Mach suddenly passed away. Henryk was an inspirational character for us and for several generations of scientists. He will be greatly missed.

[2] Present addresses: Department of Physics, Faculty of Engineering and Physical Sciences, University of Surrey Guildford, GU2 7XH, United Kingdom

crystals. The selected photomultiplier tube (PMT) is the Hamamatsu R9779, which is the most performing model available nowadays in the market [12]. The detector time response has been optimized by fine-tuning of the electronics parameters. Three crystals with different nominal Ce concentration were used [15], making it possible to assess the effect of the amount of doping on the time response. This work is part of a broader study of the characteristics of ultrafast scintillators detectors, equipped with crystals of different types, sizes and geometries and coupled to state-of-the-art photomultipliers. The aim is to construct a high performance fast-timing array of $LaBr_3$(Ce) detectors for $\gamma - \gamma$ and $\beta - \gamma$ spectroscopy, and in particular the optimal FAst TIMing array (*FATIMA*) [16], which will be placed at the focal plane of the SuperFRS at FAIR. This instrument belongs to the HISPEC-DESPEC experiment [17, 18] of the Nuclear Structure Astrophysics and Reactions (NUSTAR) collaboration, one of the four pillars of the FAIR project [19].

2. Detector characteristics

2.1. The $LaBr_3$(Ce) detectors

Three $LaBr_3$(Ce) crystals with identical shapes were studied in order to characterize their timing properties. The crystals were produced by different manufacturers with distinct Ce dopant concentration, but having the same cylindrical shape with nominal size of 1-in. in height and 1-in. in diameter, and hermetically sealed inside an aluminum housing. The housing had a thin aluminium window at the entrance, and was fitted with a glass light guide at the coupling side to the photosensor. Inside the case several layers of light reflector and shock absorbing material assure the stability of the crystal and minimize photon losses.

Crystals were labeled as *A*, *B* and *C*. Crystal *C* was the first one produced; it was grown in 2006 as a test crystal. Since it had been reported that the time resolution of $LaBr_3$(Ce) crystals improves with the amount of Ce doping [20], Crystal *C* was made with enhanced Ce doping concentration of 10%, while standard crystals were commercially available with 5% doping. Crystal *A* was produced in the same year as a commercial crystal using the standard crystal growth and production techniques, with a 5% of Ce. Finally, at the end of 2012, Crystal *B* was produced with an 8% Ce doping, with the idea of finding a good balance between increased doping and homogeneity for medium-sized crystals.

The chosen photomultiplier tube fitting the crystal properties is the Hamamatsu R9779. This tube is optimized for fast timing applications and shows good timing and energy characteristics [12, 13]. It is an 8-stage device with a window of 2 in. in diameter, equipped with bialkali photocathode. It has a typical transit time of 20 ns with transit time spread (TTS) of 250 ps, and anode rise time of 1.8 ns [21]. To favour light transmission, crystals were coupled to the PMT by Viscasil silicon grease and wrapped into opaque tape. An example of the anode pulse is plotted in Figure 1. PMT high voltages in the range of −1200 V to −1300 V were found to be optimal to provide fast-timing response while preserving good energy resolution and linearity as presented in the next sections.

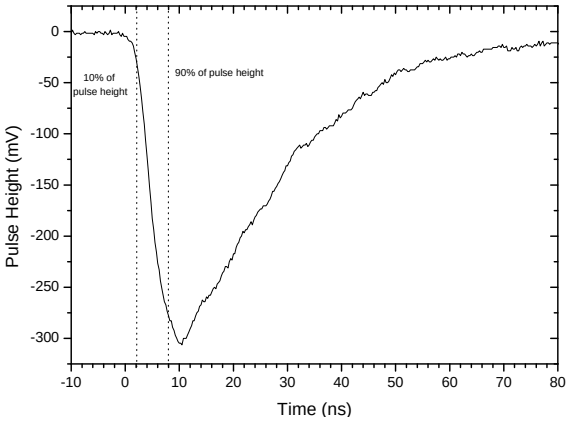

Figure 1: Anode pulse of Crystal *A*+Hamamatsu R9779 acquired with 2 Gsa/s 1 GHz oscilloscope. The used source is a standard ^{137}Cs and the PMT bias voltage −1000 V. The anode rise time taken from 10% to 90% of the maximum pulse height is ∼6 ns.

2.2. Energy resolution, linearity and efficiency

In addition to the time response, energy resolution and linearity are also important characteristics to be considered. A non-linear energy response implies high-order polynomial energy corrections, while bad energy resolution could lead to the inability of precise γ-ray energy determination and hamper transition selection.

We report here the energy resolution of Crystals *A*, *B* and *C* at 662 keV (^{137}Cs), given as the ratio between the FWHM of the γ-ray full energy peak and its energy, corrected for non-linearity [13]. The resolution was measured at the PMT bias voltages that provide the best time resolution. The relative energy resolution of Crystals *A*, *B* and *C*, once corrected for non-linearity, is measured to be 3.4%, 3.4% and 4.0% respectively. These values are worse than the number quoted by the manufacturer, 2.8% (at 662 keV), due to the use of the fast R9779 PMT [21], which is optimized for timing measurements, and provides the best timing performance at the expense of

slightly worse energy resolution. To quantify this effect Crystal *A* was also tested with a second PMT, designed for energy measurements (Hamamatsu R6231), yielding 2.9% (at 662 keV), value that matches the specifications. Table 1 summarizes the energy resolution measured for the three crystals with both PMT models (R9779 and R6231) and Figure 2 illustrates Crystal *B* energy resolution as a function of the energy in the range from 122 to 1332 keV.

Crystal	Ce (%)	PMT	HV(V)	Er (%)
A	5	R9779	1300	3.4
A	5	R6231	1000	2.9
B	8	R9779	1300	3.4
C	10	R9779	1200	4.0

Table 1: Relative energy resolution Er of the three crystals (A, B and C) at ^{137}Cs energy (662 keV). The uncertainty in the values is 0.1%. The crystals were coupled to Hamamatsu R9779 and R6231 PMTs.

The dependence of the energy resolution on the Ce concentration was assessed as well. It has been shown in [20] that up to 5% of Ce concentration the $LaBr_3$(Ce) photon yield increases [20] and hence the energy resolution also improves. However, a further Ce increase leads to constant or even lower energy resolution [22]. In our case, Crystals *A* (5% of Ce) and *B* (8% of Ce) have the same energy resolution, while Crystal *C*, with a 10% nominal Ce concentration, shows the worst value among the three, 4.0%. The measured photon yield for crystal *C* is ∼8% lower than for crystal *A*, in accordance with [20], but also the photon yield for crystal *B* with 8% Ce doping is higher than for crystal *A* by ∼10%. Given that the contributions to the intrinsic resolution are the non proportional response (which is low for $LaBr_3$(Ce) [2]) and the inhomogeneities, which cause local variations in the scintillation light output [23], the main reason for the worse energy resolution for the highly doped crystal *C* could be explained by Ce inhomogeneities in the crystal.

Detectors based on high photon yield scintillators such as $LaBr_3$(Ce) may display non-linear behaviour, even with good light yield proportionality. This may be caused by space-charge effects in the photomultiplier tube [24]. In order to check the energy linearity of our detectors, we have measured the functional relationship between the peak position (signal amplitude) and the real γ-ray energy from a ^{152}Eu source for the three crystals at bias voltages in the range from −900 V to −1700 V. We have found that $LaBr_3$(Ce) detectors behave linearly over the analysed energy range, and especially at PMT voltage values from −900 V to −1300 V. Small

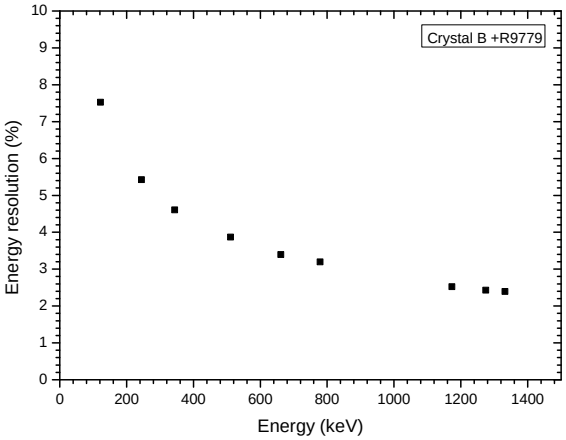

Figure 2: Energy resolution of Crystal *B*+Hamamatsu R9779 as a function of the energy. The PMT is operated at −1300 V.

deviations from linearity appear at −1300 V, where the best time resolution is achieved. At higher voltages than −1300 V the behaviour deviates significantly from linearity. It has to be noted that the three detectors have the same response, supporting the idea that the main influence comes from the PMT gain variance [23]. As an example, Figure 3 shows the signal amplitude (peak position) versus the γ-ray energy for Crystal *B* at different PMT voltages. To illustrate the departure from the linear behaviour only the first four points of each data set were linearly fitted, and the fit was extrapolated up to the 1600 keV range.

It should be underlined that at the operational voltage giving the best timing performance (see subsection 3.3), both the energy resolution and linearity of the $LaBr_3$(Ce)+R9779 detectors are also optimal, and thus well suited for spectroscopy measurements.

Another interesting feature for the design of a fast-timing array based on this kind of detectors is the γ-ray detection efficiency. In the present study the absolute full energy peak efficiency was measured with a ^{152}Eu source placed at several distances from the crystal housing end-cap. Results for Crystal B at the distances of 20, 40, 100 and 150 mm are shown in Figure 4. The crystal was coupled to the R9779 PMT, which was powered to 1300 V.

3. Description of the measurements

3.1. Experimental set-up for time-resolution measurements

The time characterization of each $LaBr_3$(Ce) detector was performed by coincidence measurements against a

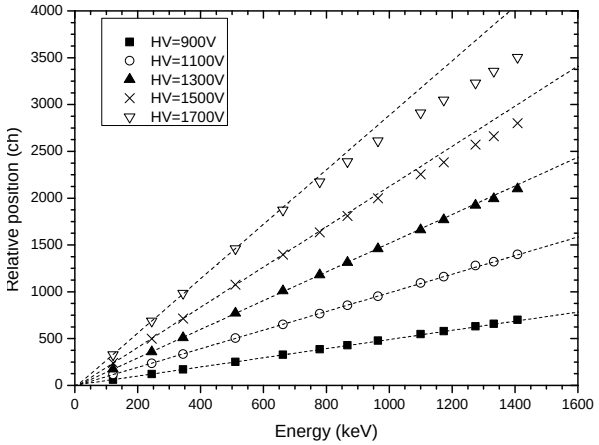

Figure 3: Functional relation between the peak position and the actual γ energy taken at five different HV values, for Crystal *B* coupled to the R9779 PMT. Only the first 4 points of each data set were linearly fitted.

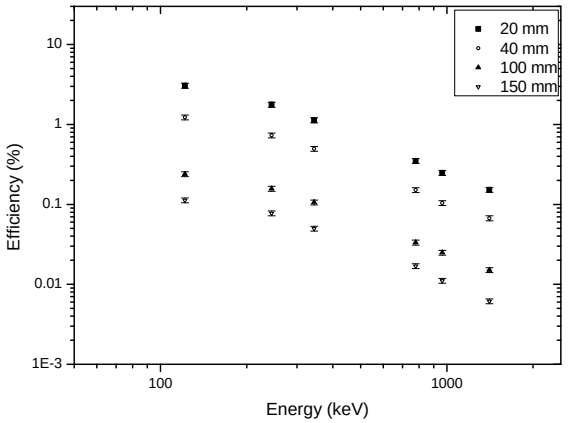

Figure 4: Full energy peak detection efficiency of Crystal B-R9779 operated at −1300 V. The γ-ray efficiency was measured at 20, 40, 100 and 150 mm from the crystal end-cup in the energy range from 122 to 1408 keV.

BaF_2 reference detector, whose time response was earlier determined by the use of three identical BaF_2 detectors with equal response [13]. Both detectors, the reference BaF_2 and the one under study, are fixed to a frame, aligned and held in close geometry, with the radioactive source placed in between. The small BaF_2 reference crystal was coupled to a Photonis XP2020-URQ PMT operated at −2300 V bias, and the three $LaBr_3$(Ce) crystals described above were coupled to the aforementioned Hamamatsu R9779 PMT. The negative anode signals from both PMTs are used for timing measurements, directly fed to an ORTEC 935 Constant Fraction Discrimination (CFD), where the timing of every signal is determined by the constant fraction or by the leading edge methods, generating an appropriate fast negative output pulses. After the ORTEC 935 both CFD outputs are sent to an ORTEC 567 Time to Amplitude Converter (TAC), which works as an time comparator, and provides square pulses whose height corresponds to the time difference between the start (BaF_2) and the stop ($LaBr_3$(Ce)) signals.

The last dynode positive signals are used for the energy measurement. They are processed firstly by an ORTEC 113 preamplifier and then by a TENNELEC TC 247 spectroscopic amplifier module.

The TAC amplitude signal and the two energy signals after the amplifier are fed to ADCs. For each valid TAC event a gate signal is generated by means of a Gate and Delay Generator enabling the acquisition and digitization in the three ADCs. Coincidence list-mode data are stored for further analysis.

3.2. Timing measurements

Timing data were collected for ^{60}Co energies and for ^{22}Na (511 keV). Data were processed and analysed with the SORTM software [25]. Since the readout electronics are very temperature sensitive, the first step of the analysis consists in the identification of shifts in the time spectrum centroids and subsequent correction. Owing to temperature stabilization, only very small variations well within the uncertainty of the centroid position, are observed. The second step consists in the offline energy gate selection on full energy peaks (FEP) at each detector, in order to project to the time spectrum for the selected energies. For the ^{60}Co source, gates are set at the 1173 and 1332-keV peaks. Thus, there are two time spectra sorted out, one for each of the two possible combinations: when the 1173-keV FEP is selected in the BaF_2 and the coincident 1332-keV FEP is detected by the $LaBr_3$(Ce) detector, and when the reversed combination is chosen. The time resolution for ^{60}Co is reported here for the summed spectrum. For the ^{22}Na source narrow gates are set at the full width at half maximum (FWHM) of the 511-keV peak, generating only one time spectrum. All steps of the sorting procedure are explained in more detail in [13, 25].

Once the time spectrum is generated, the coincidence resolution time (CRT) is obtained by measuring the FWHM of the time peak, and the individual $LaBr_3$(Ce) detector time resolution is extracted by de-convoluting the BaF_2 contribution, 81±2 ps at ^{60}Co energies and 120±2 ps at 511 keV (^{22}Na). The reported values in Table 2 refer to the individual $LaBr_3$(Ce) FWHM time resolution.

3.3. Optimization of the time resolution

The first key elements influencing the detector timing performance is the PMT itself. As discussed above, the Hamamatsu R9779 was chosen in the present work, given that it has shown much superior features than other fast PMTs also optimized for high photon yield scintillators.

The next important element is the constant fraction discriminator. In this study we used the ORTEC 935 CFD due to its proven capability of working with very fast scintillators providing excellent time resolution and time walk below ±50 ps over a 100:1 dynamic range [26]. To cope with the very short pulses and provide optimal time resolution, the ORTEC 935 CFD is equipped with an especial transformer (XFMR) for constant-fraction shaping and a selectable internal delay of −1 ns (W1). The total delay selected at the ORTEC 935 CFD determines the time of the incoming pulses, defined by the zero-crossing of the bipolar signal with the baseline. The bipolar signal originates from the addition of the attenuated signal by a factor of 20% and delayed −1 ns when W1 jumper is removed, and the original signal retarded by the CFD external delay, which is implemented as a LEMO cable at the front panel. The use in this work of very short total delays of 0.6 ns or shorter has made it possible to obtain time resolution values never achieved before.

Figure 5 sketches the operation of the ORTEC 935 module. When the external delay is shorter than 1 ns, there is no bipolar output from the XFMR and the unit works as a leading edge (LE) comparator, triggering the incoming pulses when they go above the adjusted threshold, as already discussed in [27]. Time walk, drifts and time jitter are the most common problems that deteriorate time resolution when a leading edge discriminator is used. However, when the pulse rise time is sharp enough and with low jitter, this timing triggering method can result very efficient. This issue will be explored for our 1 in. × 1 in. crystals by the operation of the ORTEC 935 in either LE or CFD mode.

In our study the time resolution was optimized through an iterative procedure, starting by the the optimization of the external CFD delay, followed by the fine tuning of the zero crossing Z, and finally of the PMT bias voltage. During the measurements the internal delay W1 jumper on the ORTEC 935 CFD was removed, setting an internal delay of −1.0 ns. We have then systematically explored a wide range of external delays from 0.5 to 20 ns. The starting value for such optimization of the external delay is the measured anode rise time at 662 keV, as depicted in Figure 1.

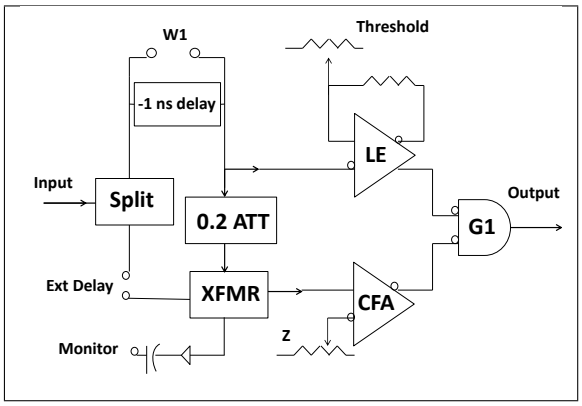

Figure 5: Simplified block diagram illustrating the operation of the ORTEC 935 CFD, adopted from [26]

Care must be taken when very short external delays like 1.5 ns are used, as the time walk becomes very sensitive to the Z value. The time resolution does not significantly change when Z is varied, but important modifications may happen on the time walk. Due to this fact, the zero crossing Z at the ORTEC 935 module was also careful investigated, firstly by observing the signals at the scope to define a valid operational range, and secondly by fine tuning the Z parameter within this range. The aim was to obtain a smooth time walk curve without compromise of the time resolution.

The final parameter to be adjusted is the PMT bias voltage, which influences the electron multiplication and collection, and secondary emissions inside the PMT. The time resolution is not as sensitive to this parameter as it is to the external delay, but it is relevant regarding the linearity and energy resolution. Space-charge effects may occur, leading to non-linear performance or affecting the energy resolution. The initial values were chosen to obtain a 1 V anode amplitude for 1 MeV incident γ-rays in the crystal. The best HV value is selected by taking into account three factors: linearity, energy resolution and time resolution.

4. Results and discussion

4.1. Dependence on the CFD external delay

The time resolution of Crystals *A*, *B* and *C* coupled to the R9779 PMT is plotted in Figure 6 for ^{60}Co energies, as a function of the ORTEC 935 CFD external delay. The best time resolutions are obtained for an external delay of 1.6 ns. For Crystal *B* (8% Ce doping) this value is as good as 98±2 ps. The best values deteriorate by more than 50% when the external delay is modified. The upper plot on Figure 6 illustrates the

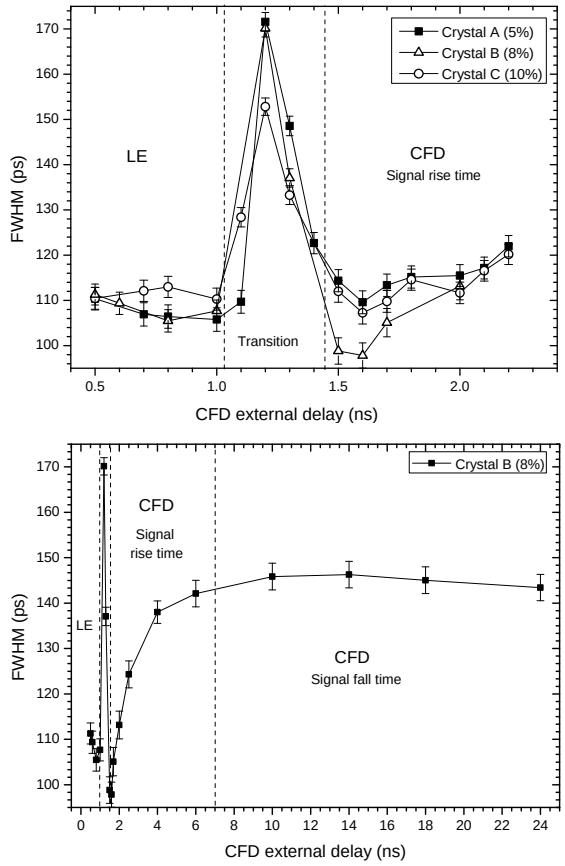

Figure 6: Time resolution of Crystals *A*, *B* and *C* as a function of the external delay, for short values (top panel). The bottom panel shows the FWHM dependence for detector *B* for the whole range of study. Detectors *A* and *B* are operated at −1300 V and *C* at −1200 V. The CFD settings correspond to Z=2.0 mV and Th=−508 mV.

FWHM versus external delay dependence in the short delay range for Crystals *A*, *B* and *C*. The bottom panel displays the FWHM as a function of the CFD external delay for Crystal B in the entire range. The trend is identical for all three detectors.

There are four distinct regions of operation of the CFD as a function of the external delay.

When the external delay is smaller than 1 ns (0.5−0.8 ns) the 935 unit triggers as a LE discriminator providing a good time resolution independently of the external delay and comparable to that obtained by the CFD triggering procedure. This is possible because the incoming pulses have a sharp rise time and show a low level of jitter. The leading edge triggering fractions were also investigated here in order to achieve the best values of FWHM time resolution. The optimal leading edge triggering level is reached when the threshold control at the ORTEC 935 is set at −508 mV, equivalent to a real input voltage level of 64 mV. At this operation bias, this corresponds to a 3.75% of the anode pulse height for γ-rays of 1332 keV.

Secondly, there is an unstable region between 0.9 and 1.3 ns where the time resolution severely increases, as a consequence of the regime transition. The operation in this mode should be avoided.

Thirdly, for external delays higher than 1.4 ns, the ORTEC 935 works correctly as a CFD discriminator. In this regime the time resolution achieves a minimum at 1.6 ns for the three crystals, and afterwards it smoothly increases until it reaches a fairly constant value of FWHM for external delays larger than 7 ns (effective shaping delay equal to the pulse rise time, 6 ns).

Finally, for long delays the CFD operates on the decay of the time pulses, yielding and almost flat behaviour of the time resolution, but at the expense of worse values, which reach (146±2 ps) at 14 ns for Crystal *B*.

4.2. Time resolution

The best time resolutions that we have obtained for Crystals *A*, *B* and *C* at ^{60}Co energies are 106±2, 98±2 and 107±2 ps respectively. These values are achieved when very short external delays around 1.6 ns are set at the ORTEC 935 and the Hamamatsu R9779 is operated in the range −1200 or −1300 V.

We note already at this point that the time resolution is not drastically affected by the PMT bias voltage. In fact the response is nearly flat. There is only a small difference in FWHM, below 5 ps, between the best and the worse values in the studied range, which varies from −1100 to −1700 V.

Crystal *B*, which was the last one produced and contains 8% of Ce dopant, provides the best value of time resolution, below 100 ps at ^{60}Co energies. The time spectra of Crystal B+R9779 is shown in Figure 7. The FWHM resolution of 190 ps using a ^{22} Na source includes the individual contributions from the reference detector of 120±2 ps and the $LaBr_3$(Ce) unit of 148±2 ps. Similarly the time resolution of 127 ps using a ^{60}Co source is the convolution of the individual reference detector resolution of 81±2 ps and that of the $LaBr_3$(Ce) detector, which is 98±2 ps.

The best FWHM values of time resolution at ^{60}Co energies and 511 keV (^{22}Na) for the three individual $LaBr_3$(Ce) crystals are summarized in Table 2. The best value for Crystal *A* (106±2 ps) is achieved when the ORTEC 935 triggers as a LE discriminator, due to the very steep pulse rise time (see Figure 1). The value increases up to 110±2 ps when the module works as CFD

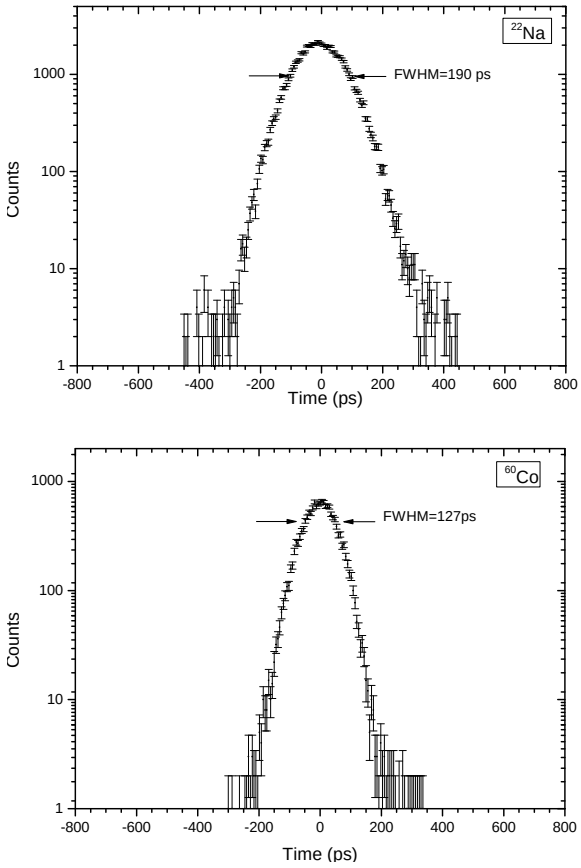

Figure 7: Time spectrum for Crystal B–R9779 detector against the reference detector measured with a ^{22}Na source (top panel). The FWHM resolution of 190 ps is the convolution of the contributions from the reference detector of 120±2 ps and the $LaBr_3$(Ce) unit of 148±2 ps. The bottom panel shows the time spectrum measured for the same detectors using a ^{60}Co source. Here the time resolution of 127 ps includes individual contributions of 81±2 ps from the reference detector and 98±2 ps from $LaBr_3$(Ce).

discriminator. For the other crystals the values in LE operation mode are close to the best CFD mode FWHM values, showing that leading edge operation is viable whenever the time walk is not relevant.

Crystal	External Delay (ns)	HV (V)	ORTEC MODE	FWHM ^{60}Co (ps)	FWHM ^{22}Na (ps)
A	1.6	1300	CFD	110±2	164±2
A	0.8	1300	LE	106±2	158±2
B	1.6	1300	CFD	98±2	148±2
C	1.6	1200	CFD	107±2	-

Table 2: Best values of FWHM time resolution for Crystals A, B and C at ^{60}Co energies. The zero crossing value (Z) is set at 2.0 mV and the CFD threshold at -508 mV

The timing properties of $LaBr_3$(Ce) detectors are influenced by the internal structure of the crystals and the Ce concentration. In contrast to the energy resolution, the time response is expected to improve when Ce is increased above 5% [20]. Crystal *B*, which contains 8% of dopant, gives a superior time resolution (about 10% better) than Crystals *A* and *C*, even though the nominal doping concentration of crystal *C* is higher (10%). In connection with the influence on the energy resolution discussed above a possible explanation may be a non-uniform distribution of the Ce inside the scintillator, since it was grown as a test crystal when the production technique was not as developed as it is now. Local variations in the scintillation light output may affect the timing response

Not only is the time resolution achieved with Crystal *B* the best among the three detectors studied in the present work, but it also stands as the best result reported to date for a standard cylindrical 1-in. $LaBr_3$(Ce) crystal [24]. This has been possible thanks to the good properties of the Hamamatsu R9779 PMT in conjunction with the use of the ORTEC 935 CFD at very short delays. The excellent time resolution of 98±2 ps at ^{60}Co energies is a step forward for the application of the ATD method in nuclear spectroscopy.

4.3. Zero crossing and time walk

The time walk optimization by the adjustment of the zero crossing potentiometer in the 935 CFD only produces minor changes in the width of the time distribution. The systematic analysis yields the best time resolution for a zero crossing parameter of Z=2.0 mV.

Obviously the Z value affects the time walk, which needs to be corrected for when the detectors are used in a real experiment in a wider energy range. Nevertheless the Compton time walk provides a good approximation of the FEP time walk when using small crystals like those under study in this paper [28]. In order to define suitable operational values, it is therefore useful to examine the time position as a function of energy for the different settings . Figure 8 shows the centroid position of the time distribution as a function of energy for Compton events arising from the 1173-keV γ-ray from ^{60}Co, for Crystals *A* (standard) and *B* (enhanced doping of 8%). As depicted in the figure positive values of Z yield a smooth behaving time walk, which can be accounted for in the measurements. At the best Z value for time resolution, the Compton walk is of the order of 300 ps over 1 MeV for Crystal *B*. Although smaller walk can be obtained at a setting of Z=1.0 mV, this is at the expense of a steeper curve at low energies. Crystal *A* has a similar behaviour, but in this case it is possible

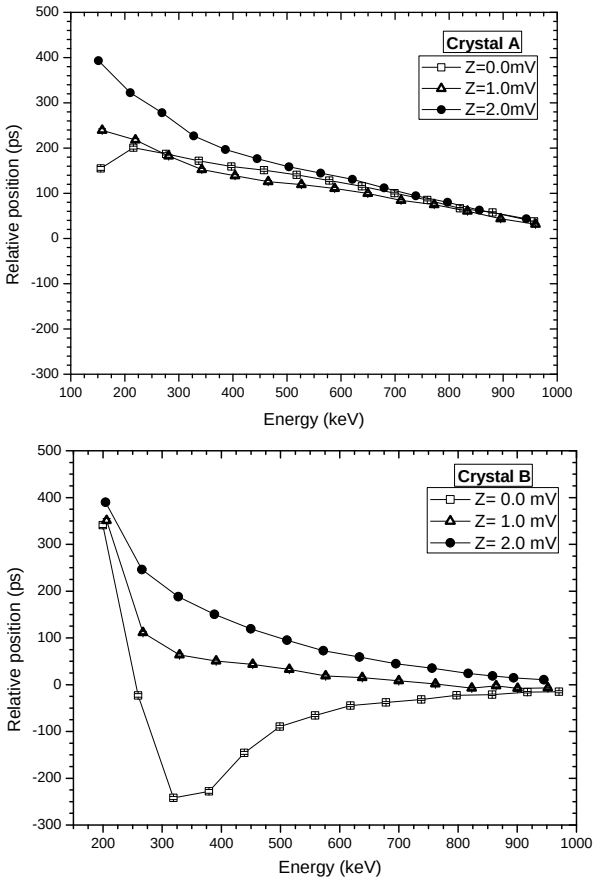

Figure 8: Compton time walk response of Crystal *A* (top panel) and *B* (bottom panel) coupled to the Hamamatsu R9779 PMT. Detectors are operated at −1300 V and the external CFD delay is set to 1.6 ns. The zero time references is given by the position of 1173-keV full energy peak.

to achieve walk of the order of 150 ps/MeV for settings Z=1.0 mV or Z=0.5 mV.

5. Summary and conclusions

We have investigated the time response of three scintillator detectors equipped with cylindrical $LaBr_3$(Ce) crystals, 1-in in height and 1-in. in diameter, produced with different nominal Ce doping. The aim of the study was to obtain the best time resolution through the optimization of the electronics parameters, while keeping the detectors good energy resolution and linearity. The crystals were tested with the Hamamatsu R9779 photomultiplier tube, which was selected due to its good timing properties, against a fast BaF_2 reference detector, at 1173-keV/1332-keV (^{60}Co) and 511-keV (^{22}Na) energies. Time signals were processed with analogue electronics by means of a 935 CFD and a 567 TAC by ORTEC. The CFD parameters were scanned and fine-tuned in order to achieve the narrowest time distribution.

We report the time resolutions at ^{60}Co energies, given as the FWHM for the individual $LaBr_3$(Ce) detector, of 106±2, 98±2 and 107±2 ps, for Crystals *A* (standard 5% Ce doping), *B* (8% Ce) and *C* (test crystal 10% Ce), respectively. The differences show the effect of the amount of Ce and the crystal structure. As expected the time resolution of of Crystal *B* (8% Ce) is better than Crystal *A* (5% Ce) [20], but, in contrast to former studies, the time resolution of Crystal *C* (10% Ce) is worse. This could be understood as inhomogeneities in the doping distribution at the time when it was manufactured as a test crystal.

We also conclude that the leading edge operation mode of the ORTEC 935 may provide similar or better values for the time resolution than the CFD operation method at a given energy. This is the case of Crystal *A* after the optimization of the triggering fraction by the modification of the threshold control value of the CFD module. For the operation in the CFD regime, the time walk has been assessed by taking advantage of the good ORTEC 935 qualities and the possibility of precise zero-crossing adjustment. We have shown that a very smooth time walk is obtained for energies lower than 1 MeV.

Finally, for Crystal *B*, with enhanced Ce doping of 8%, we have found that a bias voltage of −1300 V on the PMT, together with the optimal CFD parameters of Z= 2.0 mV and external delay of 1.6 ns, yield the best time resolutions at ^{60}Co and ^{22}Na energies. The time resolution measured at ^{60}Co energies has been pushed below 100 ps to 98±2 ps, which should be compared to the best resolution available to date with a similar cylindrical 1-in. $LaBr_3$(Ce) crystal of 107±4 ps, reported by Moszyński *et al.*, using the Photonis XP20D0 PMT [24]. This improved time resolution represents and advancement for the application of the fast-timing ATD method.

In conclusion we have shown that, apart from crystal and photomultiplier selection, the optimization of electronic parameters leads to improved time resolution for standard 1-in. $LaBr_3$(Ce) detectors. This work will be extended further by studying larger crystals and different geometries, which are of relevance for the construction of the FAst TIMing Array (FATIMA) for studies of nuclei far off the line of stability.

Acknowledgements

This work was partially supported by the Spanish MINECO through projects FPA2010-17142, FPA2013-

41267-P and Consolider-CPAN CSD-2007-00042. Funding by the ERA-NET NuPNET via Spanish project PRI-PIMNUP-2011-1338 (FATIMA-NuPNET) and Bulgarian project DNS7RP01-4 (FATIMA-NuPNET) is also recognized. V.V. and H.M. acknowledge the financial aid by the Consolider-CPAN CSD-2007-00042 project. The electronics for the test bench and the reference detectors were provided by the Fast Timing Pool of Electronics and MASTICON.

Bibliography

References

[1] E. V. V. Loef, P. Dorenbos, C. W. E. van Ejik, K. Krämer, H. U. Güdel, Scintillation properties of LaBr3:Ce3+ crystals: Fast, efficient and high-energy-resolution scintillators, Nuclear Instruments and Methods in Physics Research A 486 (2002) 254–258.

[2] K. Shah, J. Glodo, M. Klugerman, W. Moses, S. Derenzo, M. Weber, $LaBr_3$:Ce scintillators for Gamma-Ray spectroscopy, IEEE Transactions on Nuclear Science 50 (6) (2003) 2410–2413. doi:10.1109/TNS.2003.820614.

[3] S. Gobain, Brillance 380 Brochure.

[4] P. Dorenbos, Light output and energy resolution of Ce^{3+}-doped scintillators, Nuclear Instruments and Methods in Physics Research Section A 486 (2002) 208–213.

[5] E. R. White, H. Mach, L. M. Fraile, U. Köster, O. Arndt, A. Blazhev, N. Boelaert, M. J. G. Borge, R. Boutami, H. Bradley, N. Braun, Z. Dlouhy, C. Fransen, H. O. U. Fynbo, C. Hinke, P. Hoff, A. Joinet, A. Jokinen, Lifetime measurement of the 167.1 keV state in ^{41} Ar, Physical Review C 057303 (2007) 7–10. doi:10.1103/PhysRevC.76.057303.

[6] H. Mach, R. L. Gill, M. Moszyński, A method for picosecond lifetime measurements for neutron-rich nuclei (1) Outline of the method, Nuclear Instruments and Methods in Physics Research A 280 (1989) 49–72.

[7] M. Moszyński, H. Mach, A method for picosecond lifetime measurements for neutron-rich nucleI (2) Timing study with scintillation counters, Nuclear Instruments and Methods in Physics Research A 277 (1989) 407–417.

[8] N. Mărginean, D. Balabanski, D. Bucurescu, S. Lalkovski, L. Atanasova, G. Căta-Danil, I. Căta-Danil, J. Daugas, D. Deleanu, P. Detistov, G. Deyanova, D. Filipescu, G. Georgiev, D. Ghiţă, K. Gladnishki, R. Lozeva, T. Glodariu, M. Ivaşcu, S. Kisyov, C. Mihai, R. Mărginean, A. Negret, S. Pascu, D. Radulov, T. Sava, L. Stroe, G. Suliman, N. Zamfir, In-beam measurements of sub-nanosecond nuclear lifetimes with a mixed array of HPGe and $LaBr_3$Ce detectors, The European Physical Journal A 46 (3) (2010) 329–336. doi:10.1140/epja/i2010-11052-7.

[9] T. Alharbi, P. H. Regan, P. J. R. Mason, N. Mărginean, Z. Podolyák, A. M. Bruce, E. C. Simpson, A. Algora, N. Alazemi, R. Britton, M. R. Bunce, D. Bucurescu, N. Cooper, D. Deleanu, D. Filipescu, W. Gelletly, D. Ghiţă, T. Glodariu, G. Ilie, S. Kisyov, J. Lintott, S. Lalkovski, S. Liddick, C. Mihai, K. Mulholland, R. Mărginean, A. Negret, M. Nakhostin, C. R. Nita, O. J. Roberts, S. Rice, J. F. Smith, L. Stroe, T. Sava, C. Townsley, E. Wilson, V. Werner, M. Zhekova, N. V. Zamfir, Electromagnetic transition rates in the N=80 nucleus $^{138}_{58}$Ce, Phys. Rev. C 87 (2013) 014323. doi:10.1103/PhysRevC.87.014323.

[10] B. Olaizola, L. M. Fraile, H. Mach, A. Aprahamian, J. A. Briz, J. Cal-González, D. Ghiţă, U. Köster, W. Kurcewicz, S. R. Lesher, D. Pauwels, E. Picado, A. Poves, D. Radulov, G. S. Simpson, J. M. Udías, β^-decay of ^{65}Mn to ^{65}Fe, Phys. Rev. C 88 (2013) 044306. doi:10.1103/PhysRevC.88.044306.

[11] J.-M. Régis, G. Simpson, A. Blanc, G. de France, M. Jentschel, U. Köster, P. Mutti, V. Paziy, N. Saed-Samii, T. Soldner, C. Ur, W. Urban, A. Bruce, F. Drouet, L. Fraile, S. Ilieva, J. Jolie, W. Korten, T. Kröll, S. Lalkovski, H. Mach, N. Marginean, G. Pascovici, Z. Podolyak, P. Regan, O. Roberts, J. Smith, C. Townsley, A. Vancraeyenest, N. Warr, Germanium-gated $\gamma - \gamma$ fast timing of excited states in fission fragments using the exill-fatima spectrometer, Nuclear Instruments and Methods in Physics Research Section A: Accelerators, Spectrometers, Detectors and Associated Equipment 763 (0) (2014) 210 – 220. doi:http://dx.doi.org/10.1016/j.nima.2014.06.004.

[12] L. M. Fraile, H. Mach, B. Olaizola, V. Paziy, E. Picado, J. J. Sanchez, J. M. Udías, J. J. Vaquero, V. Vedia, Assessment of new photosensors for fast timing applications with large scintillator detectors, in: Nuclear Science Symposium and Medical Imaging Conference (NSS/MIC), 2011 IEEE, 2011, pp. 72 –74. doi:10.1109/NSSMIC.2011.6154403.

[13] L. M. Fraile, H. Mach, V. Vedia, B. Olaizola, V. Paziy, E. Picado, J. Udías, Fast timing study of a $CeBr_3$ crystal: Time resolution below 120 ps at ^{60}Co energies, Nuclear Instruments and Methods in Physics Research Section A: Accelerators, Spectrometers, Detectors and Associated Equipment 701 (0) (2013) 235 – 242. doi:http://dx.doi.org/10.1016/j.nima.2012.11.009.

[14] L. M. Fraile, H. Mach, E. Picado, V. Vedia, J. Udías, Study of the time response of a LuAG(Pr) crystal for fast timing applications, Nuclear Instruments and Methods in Physics Research Section A: Accelerators, Spectrometers, Detectors and Associated Equipment 713 (0) (2013) 27 – 32. doi:http://dx.doi.org/10.1016/j.nima.2013.02.015.

[15] V. Vedia, H. Mach, L. M. Fraile, J. M. Udías, Optimization of the Time Response of $LaBr_3$(Ce) Crystals, and its Dependence on Ce Concentration, in: JPS Conference Proceedings. ARIS 2014, Vol. Volume 6, 2015.

[16] L. M. Fraile, et.al, Technical Design Report for the DESPEC Fast Timing Array, unpublished (2015).

[17] B. Rubio, Z. Podolyák, M. Górska, J. Gerl, W. Korten, Fair-experiments-26 decay spectroscopy DESPEC at the new FAIR-NUSTAR facility.

[18] Zsolt Podolyák, From RISING to HISPEC-DESPEC, Nuclear Instruments and Methods in Physics Research Section B: Beam Interactions with Materials and Atoms 266 (19-20) (2008) 4589–4594, proceedings of the XVth International Conference on Electromagnetic Isotope Separators and Techniques Related to their Applications. doi:http://dx.doi.org/10.1016/j.nimb.2008.05.106.

[19] FAIR, Facility for Antiproton and Ion Research in Europe, Planckstr. 1, 64291 Darmstadt, Germany. www.gsi.de/en/research/fair.htm.

[20] J. Glodo, W. W. Moses, W. M. Higgins, E. V. D. V. Loef, P. Wong, S. E. Derenzo, M. J. Weber, K. S. Shah, Effects of Ce Concentration on Scintillation Properties of $LaBr_3$(Ce), IEEE Transactions on Nuclear Science 52 (5) (2005) 1805–1808.

[21] Hamamatsu Photonics, Photomultiplier Tube R9779 Specifications (2009).

[22] W. Drozdowski, P. Dorenbos, A. J. J. Bos, G. Bizarri, A. Owens, F. G. A. Quarati, $CeBr_3$ Scintillator Development for Possible Use in Space Missions, IEEE Transactions on Nuclear Science 55 (3) (2008) 1391–1396.

[23] P. Dorenbos, J. de Haas, C. van Eijk, Non-proportionality in the scintillation response and the energy resolution obtainable with scintillation crystals, Nuclear Science, IEEE Transactions on 42 (6) (1995) 2190–2202. doi:10.1109/23.489415.

[24] M. Moszyński, M. Gierlik, M. Kapusta, A. Nassalski, T. Szczęśniak, C. Fontaine, P. Lavoute, New photonis XP20D0 photomultiplier for fast timing in nuclear medicine, Nuclear Instruments and Methods in Physics Research Section A: Accelerators, Spectrometers, Detectors and Associated Equipment 567 (1) (2006) 31–35, proceedings of the 4th International Conference on New Developments in Photodetection BEAUNE 2005 Fourth International Conference on New Developments in Photodetection. doi:http://dx.doi.org/10.1016/j.nima.2006.05.054.

[25] H. Mach, Instructions for the program SORTM, Internal Report. Universidad Complutense, 2012.

[26] Model 935 Quad Constant-Fraction 200-MHz Discriminator Operating and Service Manual.

[27] T. Szczesniak, M. Moszynski, A. Nassalski, P. Lavoute, A. Dehaine, A further study of timing with LSO on XP20D0 for TOF PET, IEEE Transactions on Nuclear Science 54 (5) (2007) 1464–1473. doi:10.1109/TNS.2007.906406.

[28] H. Mach, F. Wohn, G. Molnár, K. Sistemich, J. C. Hil, M. Moszyński, R. Gill, W. Krips, D. Brenner, Retardation of B (E2: $0_1^+ \rightarrow 2_1^+$) rates in $^{90-96}Sr$ and strong subshell closure effects in the A ∼100 region, Nuclear Physics A 523 (2) (1991) 197 – 227". doi:http://dx.doi.org/10.1016/0375-9474(91)90001-M.
URL